Electronic Supplementary Material (ESI) for Materials Chemistry Frontiers.

Supplementary Information for

Enhanced production of aromatics from syngas over CoMnAl oxides combined with *b*-axis thickness tailored HZSM-5

Ruixin Guo[1,2,†], Jia Liu[1,2,†], Hao Wang[1,2*], Xing Yu[1], Jian Zhang[1], Chengguang Yang[1,2*], Jiong Li[3], Yuhan Sun[4], Peng Gao[1,2*]

[1] CAS Key Laboratory of Low-Carbon Conversion Science and Engineering, Shanghai Advanced Research Institute, Chinese Academy of Sciences, Shanghai 201210, China

[2] University of Chinese Academy of Sciences, Beijing 100049, China

[3]Shanghai Synchrotron Radiation Facility, Shanghai Advanced Research Institute, Chinese Academy of Sciences, Shanghai 201204, China

[4]School of Physical Science and Technology, ShanghaiTech University, Shanghai 201210, China

[†] These authors contributed equally: Ruixin Guo, Jia Liu.

* Corresponding author. Email: haowang@sari.ac.cn, yangcg@sari.ac.cn, gaopeng@sari.ac.cn.

S1. Methods

S1.1 Catalyst characterizations

X-ray diffraction (XRD) analyzer (Rigaku Ultima IV) was used to record the XRD patterns of the samples. The ratio of Si/Al was determined by X-ray fluorescence (XRF) using a Rigaku ZSX Primus II instrument.

Emission scanning electron microscopy (SEM) (ZEISS SUPRRATM55 SAPPHIRE) and transmission electron microscopy (TEM) (JEOL-JEM 2000FX) were used for morphological observation. The samples were dispersed in ethanol following ultra-sonication and then dropped on a carbon-coated copper grid for measurement.

N_2 pysisorption was carried out on the Micromeritics ASAP 3020 instrument. The sample was firstly degassed at 200 °C in a vacuum for 12 h and then moved to the analysis station for adsorption-desorption at −196 °C. The specific surface area was determined based on the Brunauer-Emmett-Teller (BET) method and the pore volume and pore diameter were calculated based on the Barrett-Joyner-Halenda (BJH) model.

X-ray photoelectron spectroscopy (XPS) was collected on a Thermo Scientific K-Alpha with Al Kα at 150 W (hv = 1486.6 eV) under 5×10^{-7} Pa, calibrated internally by the carbon deposit C1s (E_b = 284.8 eV).

^{27}Al MAS NMR experiments were tested on Bruker AVANCE III 600 spectrometers at 156.4 MHz with a MAS probe at a spinning rate of 14 kHz. 1.0 M $Al(NO_3)_3$ solution was referenced to the chemical shift of ^{27}Al.

NH_3 temperature-programmed desorption (NH_3-TPD) experiments were recorded with a thermal conductivity detector (TCD). Typically, 100 mg sample was pretreated in an Ar flow (30 mL·min^{-1})

at 200 °C for 1 h. After cooling to 50 °C, the sample was saturated with ammonia flow for 0.5 h, and then the Ar flow was introduced as the sweep gas. Finally, NH_3-TPD was presented in the temperature range from 50 to 600 °C at a rate of 10 °C.

X-ray adsorption near-edge spectroscopy (XANES) experiments were performanced at BL11B in Shanghai synchrotron Radiation Facility (SSRF) in transmission mode. The XANES spectra of the samples were recorded at the Co K-edge (7712 eV) under ambient conditions.

S1.2 Catalytic performance measurements

Syngas conversion was carried out on a continuous flow fixed-bed reactor under mild reaction conditions (280 °C, 2.0 MPa, 2000 $mL \cdot h^{-1} \cdot g^{-1}$ and H_2/CO ratio = 1). The calcined CMA and the ZSM-5 zeolites were ground and sieved through a 40–60 mesh. By granule mixing of 0.33 g CMA and 0.67 g ZSM-5, 1.0 g catalyst was loaded into the middle of a stainless steel autoclave. Before the reaction, the catalysts were in situ reduced at 300 °C for 8 h under 10% H_2/Ar flow (200 $mL \cdot min^{-1}$) at 0.1 MPa. Then, the reactor was cooled to the desired temperature under the reduction atmosphere and the feed gas was introduced into the reactor. After passing through a hot trap (120 °C) and a cold trap (0 °C), the tail gas products were analyzed online using a Shimadzu GC-2010. H_2, N_2, CO, CH_4, and CO_2 were detected using a thermal conductivity detector equipped with a TDX-01 column. A flame ionization detector equipped with a KCl-modified alumina capillary column was used to analyze the C1–C6 hydrocarbons. The collected liquid products were analyzed on two Shimadzu GC-2010 systems equipped with an HP-5 and an HP-innowax capillary column, respectively. CO conversion was calculated by the internal standard method using N_2 from the feed gas. Calculations of CO_2 selectivity and hydrocarbon product distribution were based on a molar carbon basis and the carbon balance was kept among 97–100%.

S2. Results and discussions

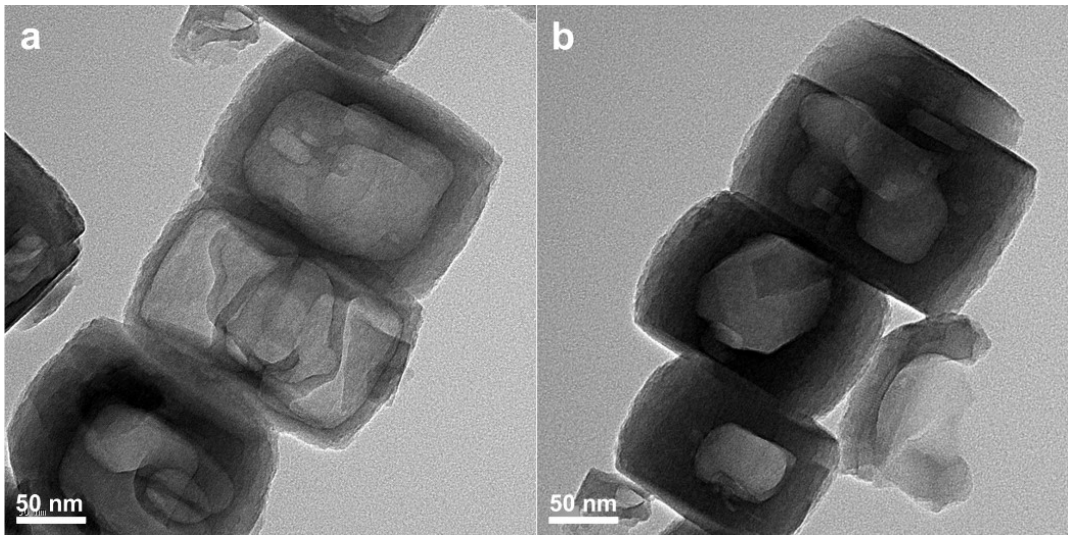

Fig. S1 TEM images of the Hol-HZ5 (a and b).

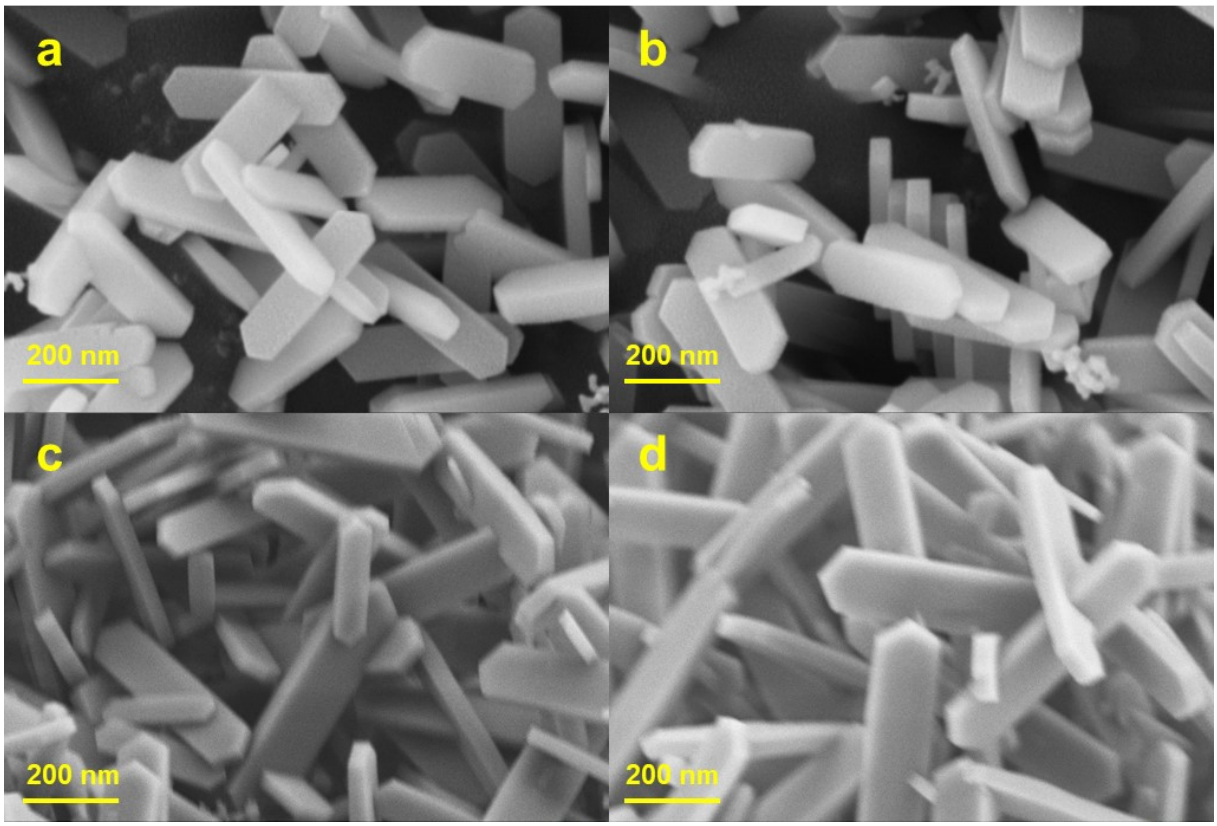

Fig. S2 SEM images of the Sbx-HZ5-65 (a), Sbx-HZ5-82 (b), Sbx-HZ5-123 (c), and Sbx-HZ5-252 (d).

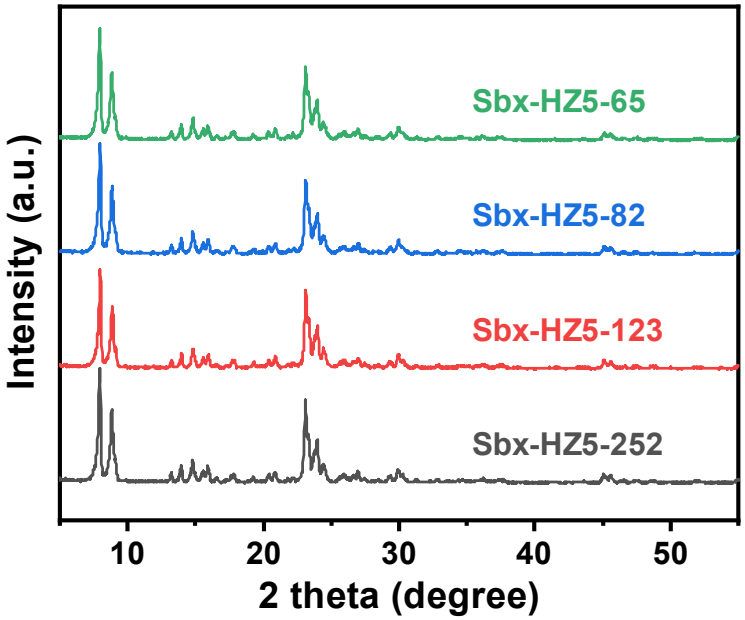

Fig. S3 XRD patterns of Sbx-HZ5 with different Si/Al molar ratio.

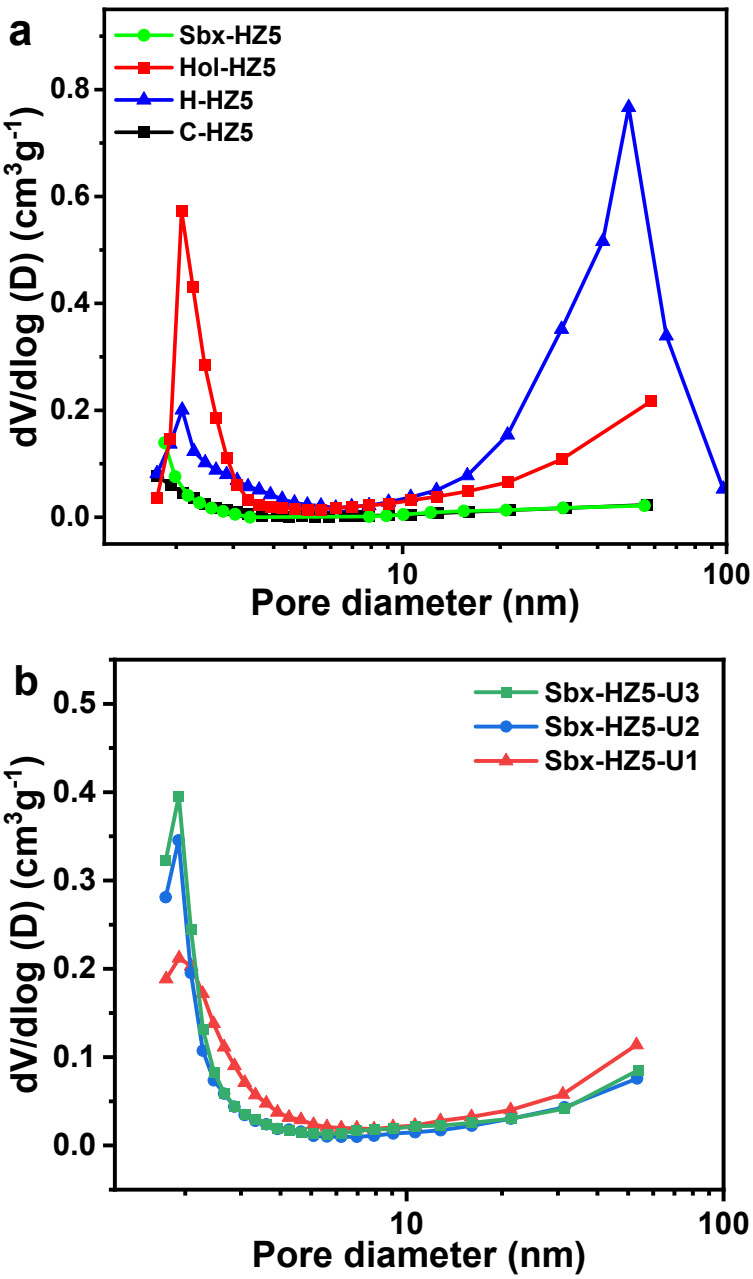

Fig. S4 The pore size distribution curves of different types of zeolites (a) and Sbx-HZ5-Uy (b).

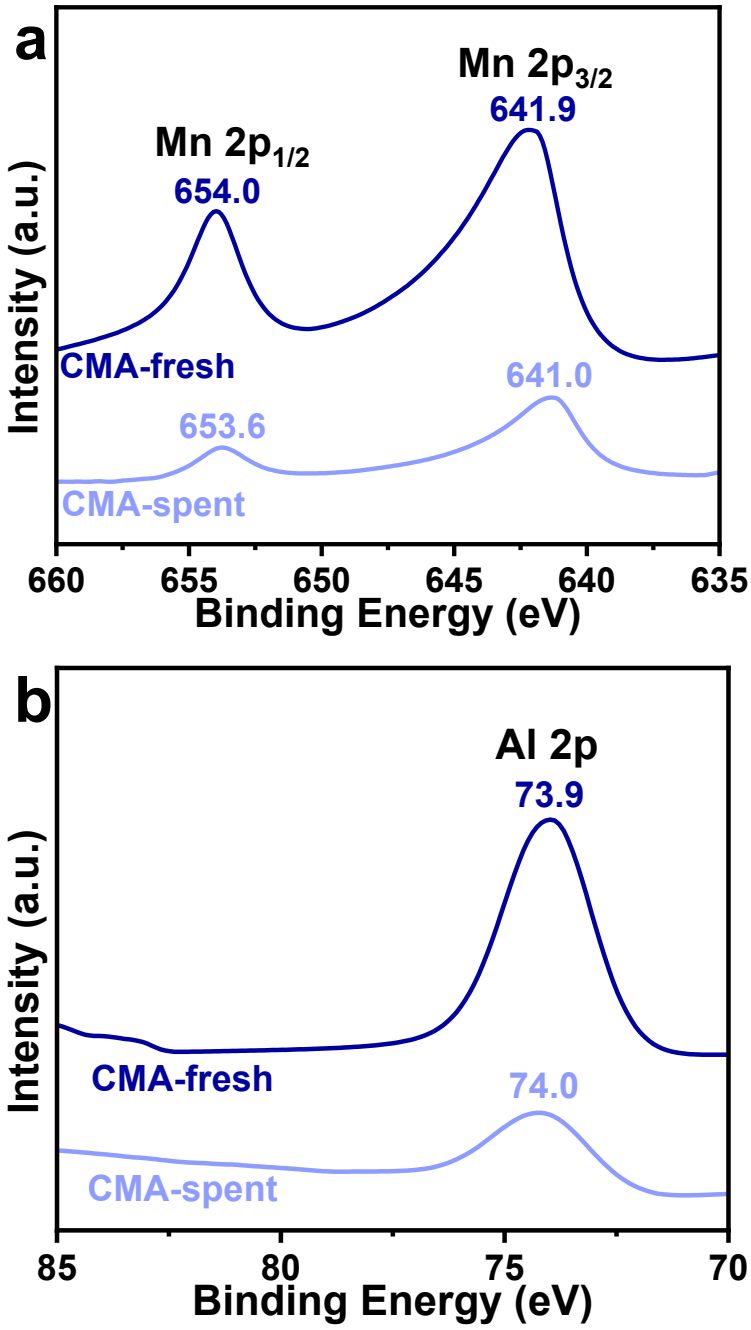

Fig. S5 Mn 2p (a) and Al 2p (b) for XPS of fresh and spent CMA catalysts.

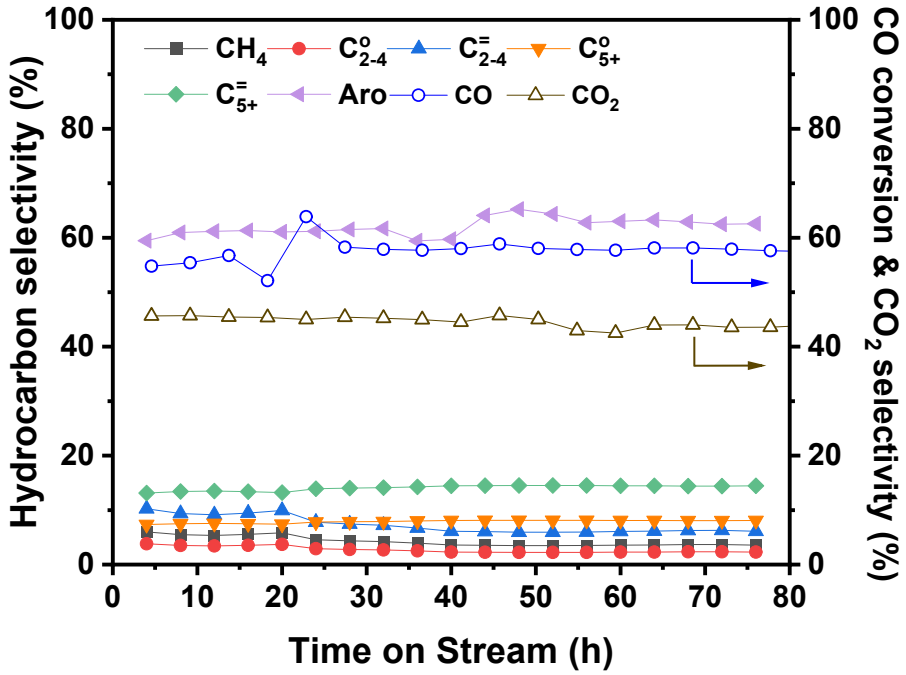

Fig. S6 Stability test of the CMA/Sbx-HZ5-123 under the standard reaction conditions.

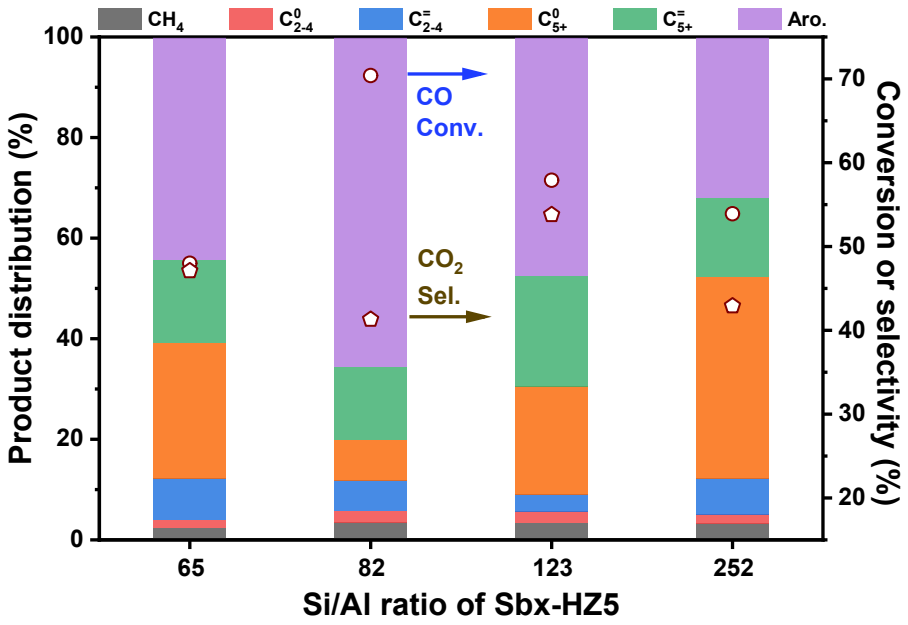

Fig. S7 The effect of Si/Al ratio of Sbx-HZ5 on the catalytic performance over bifunctional catalysts under the standard conditions.

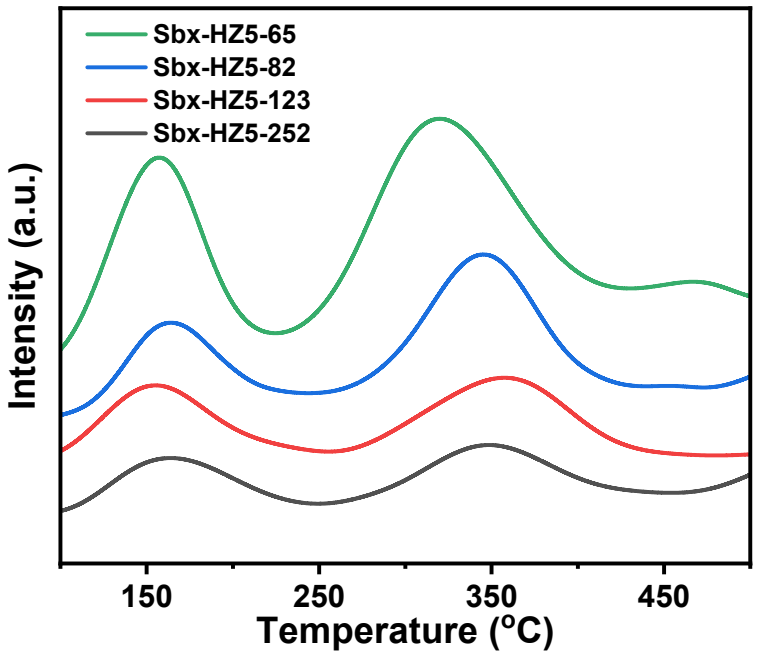

Fig. S8 NH_3-TPD profiles of the Sbx-HZ5 zeolites with different Si/Al ratio.

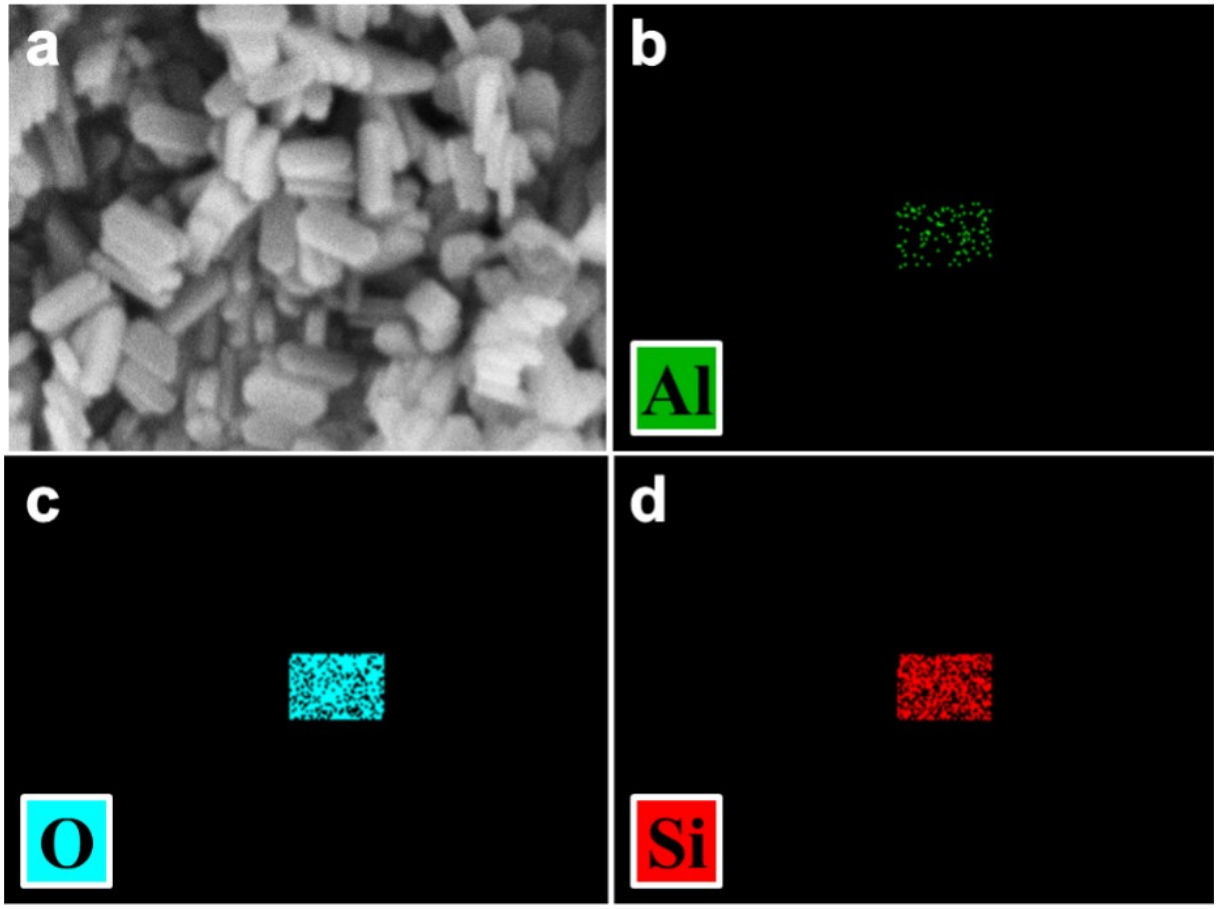

Fig. S9 SEM (a) and EDX elemental maps of Al (b), O (c), and Si (d) of Sbx-HZ5-U2.

Table S1. Catalytic performance of syngas conversion over CMA and CMA/HZSM-5 bifunctional catalysts under the standard reaction conditions.

Catalysts	CO Conv. (%)	CO_2 Sel. (%)	Product Selectivity (%)						Aro. Yield (%)
			CH_4	C_{2-4}^{o}	$C_{2-4}^{=}$	C_{5+}^{o}	$C_{5+}^{=}$	Aro.	
CMA	38.4	44.7	2.7	2.9	38.5	17.3	38.6	0	0
CMA/C-HZ5	33.5	38.1	2.1	1.8	7.9	29.1	24.5	34.6	7.2
CMA/H-HZ5	46.1	40.4	2.2	1.6	7.9	22.2	14.8	51.3	14.1
CMA/Hol-HZ5	54.5	44.3	2.7	2.1	6.1	13.8	24.9	50.3	15.3
CMA/Sbx-HZ5	57.9	53.8	3.3	2.3	3.4	21.5	22.0	47.5	12.7
CMA/Sbx-HZ5-U1	57.8	49.3	2.6	1.6	5.9	25.9	18.2	45.7	13.4
CMA/Sbx-HZ5-U2	70.4	41.3	3.5	2.3	6.0	8.1	14.5	65.6	27.1
CMA/Sbx-HZ5-U3	26.7	47.9	2.6	4.6	0.3	11.1	22.3	59.1	8.2

Reaction condition: 280 ^{o}C, 2.0 MPa, 2000 $mL \cdot g^{-1} \cdot h^{-1}$, and $H_2/CO = 1$.

Table S2. The aromatics distribution over CMA and CMA/HZSM-5 bifunctional catalysts under the standard reaction conditions.

Catalysts	Selectivity in aromatics (%)					
	B	T	E+X	C_9	C_{10}	C_{11+}
CMA	/	/	/	/	/	/
CMA/C-HZ5	6.5	8.9	25.0	14.1	18.3	27.3
CMA/H-HZ5	0.3	6.7	29.3	28.5	22.7	12.6
CMA/Hol-HZ5	6.0	10.8	21.0	23.8	16.2	22.2
CMA/Sbx-HZ5	2.6	2.5	18.9	20.1	32.8	23.1
CMA/Sbx-HZ5-U1	2.3	2.9	27.3	24.3	32.9	10.4
CMA/Sbx-HZ5-U2	0.3	3.4	24.1	28.5	20.0	23.7
CMA/Sbx-HZ5-U3	2.3	8.0	31.5	24.7	20.1	13.4

Reaction condition: 280 ^{o}C, 2.0 MPa, 2000 $mL \cdot g^{-1} \cdot h^{-1}$, and $H_2/CO = 1$.

Table S3. Comparison of reported work on syngas conversion to aromatics.

Catalysts	T (^oC)	P (MPa)	GHSV ($mL \cdot g^{-1} \cdot h^{-1}$)	CO Conv. (%)	CO_2 Sel. (%)	CH_4 Sel. (%)	Aro. Sel. (%)	Ref.
CMA/Sbx-HZ5-U2	280	2.0	2000	70.4	41.3	3.5	65.6	This work
CMA/Hol-Z5-N@2S1	280	2.0	1000	70.7	41.8	2.9	63.5	1
FeMn+HZSM-5	320	1.0	3600	43.0	33.2	21.8	31.5	2
FeMn@MZ5	320	2.0	3000	51.9	36.6	~20.0	47.1	3
$ZnCr_2O_4$-400&H-ZSM-5	390	3.0	1500	32.6	46.9	2.1	76.0	4
MnCr-Z5	430	4.0	2250	12.2	47.3	6.9	64.7	5
$ZnCrO_x$+HZSM-5	350	4.0	1500	16.0	46.9	1.7	73.9	6
Zn-ZrO_2+HZSM-5	400	3.0	500	21.0	42.0	2.2	81.0	7
Cr_2O_3/HZSM-5	395	4.0	2000	14.4	43.2	2.8	84.7	8
Fe/$ZnCr_2O_4$+HZSM-5	380	4.0	1500	57.5	~47	~3	74	9
Mo-ZrO_2+HZSM-5	400	3.0	3000	22.0	41.0	3.4	76.0	10

References

1. H. Wang, P. Gao, S. Li, T. Wang, C. Yang, J. Li, T. Lin, L. Zhong and Y. Sun, Bifunctional catalysts with versatile zeolites enable unprecedented para-xylene productivity for syngas conversion under mild conditions, *Chem Catal.*, 2022, **2**, 779–796.

2. T. Wang, Y. B. Xu, C. M. Shi, F. Jiang, B. Liu and X. H. Liu, Direct production of aromatics from syngas over a hybrid FeMn Fischer-Tropsch catalyst and HZSM-5 zeolite: Local environment effect and mechanism-directed tuning of the aromatic selectivity, *Catal. Sci. Technol.*, 2019, **9**, 3933–3946.

3. Y. Xu, G. Ma, J. Bai, Y. Du, C. Qin and M. Ding, Yolk@shell FeMn@hollow HZSM-5 nanoreactor for directly converting syngas to aromatics, *ACS Catal.*, 2021, **11**, 4476–4485.

4. Y. Fu, Y. Ni, W. Cui, X. Fang, Z. Chen, Z. Liu, W. Zhu and Z. Liu, Insights into the size effect of $ZnCr_2O_4$ spinel oxide in composite catalysts for conversion of syngas to aromatics, *Green Energy Environ.*, 2023, **8**, 530–537.

5. D. Y. Miao, Y. Ding, T. Yu, J. Li, X. L. Pan and X. H. Bao, Selective synthesis of benzene, toluene, and xylenes from syngas, *ACS Catal.*, 2020, **10**, 7389–7397.

6. J. H. Yang, X. L. Pan, F. Jiao, J. Li and X. H. Bao, Direct conversion of syngas to aromatics, *Chem. Commun.*, 2017, **53**, 11146–11149.

7. K. Cheng, W. Zhou, J. C. Kang, S. He, S. L. Shi, Q. H. Zhang, Y. Pan, W. Wen and Y. Wang, Bifunctional catalysts for one-step conversion of syngas into aromatics with excellent selectivity and stability, *Chem*, 2017, **3**, 334–347.

8. C. Liu, J. J. Su, S. Liu, H. B. Zhou, X. H. Yuan, Y. C. Ye, Y. Wang, W. Q. Jiao, L. Zhang, Y. Q. Lu, Y. D. Wang, H. Y. He and Z. K. Xie, Insights into the key factor of zeolite morphology on

the selective conversion of syngas to light aromatics over a Cr_2O_3/ZSM-5 catalyst, *ACS Catal.*, 2020, **10**, 15227–15237.

9. Y. Fu, Y. M. Ni, Z. Y. Chen, W. L. Zhu and Z. M. Liu, Achieving high conversion of syngas to aromatics, *J. Energy Chem.*, 2022, **66**, 597–602.

10. W. Zhou, S. Shi, Y. Wang, L. Zhang, Y. Wang, G. Zhang, X. Min, K. Cheng, Q. Zhang, J. Kang and Y. Wang, Selective conversion of syngas to aromatics over a Mo−ZrO_2/H-ZSM-5 bifunctional catalyst, *ChemCatChem*, 2019, **11**, 1681–1688.